2016 IEEE 55th Conference on Decision and Control (CDC)
ARIA Resort & Casino
December 12-14, 2016, Las Vegas, USA

Sparsity-Promoting Dynamic Mode Decomposition for Systems with Inputs

Jennifer Annoni, Peter Seiler, and Mihailo R. Jovanović

Abstract— **The objective of this paper is to address the selection of dominant modes of a system that can be used to construct a reduced-order model. This work is motivated by high-fidelity computational models that capture fluid and/or structural dynamics, which are prohibitively complex for real-time control. A variety of techniques for obtaining simplified control-oriented models have been developed, e.g. proper orthogonal decomposition (POD) and dynamic mode decomposition. In this paper, we address the challenge of selecting a few dominant Koopman modes for systems with exogenous inputs. We use a linear channel flow example to demonstrate the utility of our approach and illustrate the advantages relative to alternative techniques for control-oriented modeling.**

I. Introduction

Many fluid systems can be represented by a set of low-order dynamics that dominate the evolution of the flow field. By extracting the dominant characteristics of the system, low-dimensional models can be constructed that capture these dominant characteristics while maintaining computational efficiency. This work is motivated by the control of these systems that involve fluid and/or structural dynamics. One example involves the control of wind farms. The overall performance of a wind farm can be improved through proper coordination of turbines [1]. High-fidelity, computational models exist for this application [2], [3], but are prohibitively complex for control design. A second example involves the control of flexible aircraft. More fuel efficient aircraft can be designed by reducing structural weight thus leading to increased flexibility [4]. The vibrational modes can significantly degrade the performance and can even lead to aeroelastic instabilities (flutter) [4], [5]. High-fidelity, computational fluid/structural models also exist for this application [6], but these are also too complex for control design. Simplified, control-oriented models are needed in these examples.

A variety of reduced-order modeling techniques have been developed by the fluid dynamics and controls communities. These methods range from analytical reduced-order modeling, such as balanced truncation [7], to data-driven reduced-order modeling such as system identification [8] where a low-dimensional system is identified to describe the dynamics of a high-dimensional system. In the fluid dynamics literature, proper orthogonal decomposition (POD) is a standard method where the state is projected onto a low-dimensional subspace of POD modes constructed using data from high-order systems [9]–[11]. The POD modes provide the dominant spatial modes of the flow field and contain multi-frequency content. There have been variations of this method including balanced POD [12], [13] where a control-oriented model is obtained by taking the POD modes of a linearized forward simulation model and its adjoint. The adjoint of the model is used to obtain balanced POD modes that better represent the system by taking into consideration the effect of forcing inputs and measuring outputs of the system. The drawback to this approach is that the adjoint is necessary to obtain the balanced POD modes. In many cases, obtaining the adjoint is non-trivial and not available for experiments such as particle image velocimetry [14]. Dynamic mode decomposition (DMD) was developed to build upon POD by extracting the single frequency information from spatial modes. DMD fits time-domain data with linear dynamics on a reduced-order subspace [15]–[17]. This approach has ties to the Koopman operator [18]–[20].

Additional variations of DMD have been proposed in the literature to better identify the dynamics of the system. For example, DMD has been extended to streaming datasets to handle large amounts of data [21]. Various corrections for DMD have been proposed to account for noise or nonlinearities in the system by using a statistical approach [22] and using a Kalman filtering approach [23]. Sparsity-promoting DMD was proposed in [24] to better capture the dominant dynamics of the system by attempting to exclude the structures identified by standard DMD that weakly contribute to the flow. This approach is used for autonomous (unforced) systems. Recent work has been done to extend DMD, termed DMD with control (DMDc) [25], to construct reduced-order models with control inputs.

This paper presents an extension of the sparsity-promoting DMD technique to include inputs. This technique builds on a variation of DMDc [25] and sparsity-promoting DMD [24], described in Section II. In particular, it will be shown, in Section II-B, that the selection of DMD modes is dependent on the choice of exogenous input. Similar to sparsity-promoting DMD, an optimization problem is formulated using a regularization term and alternating direction method of multipliers (presented in Section II-C). The main difference in this approach is the use of block sparsity in this optimization [26]. Finally, this approach will be applied to

This work was partially supported by the National Science Foundation under Grant No. CMMI-1254129 entitled "CAREER: Probabilistic Tools for High Reliability Monitoring and Control of Wind Farms." The first author gratefully acknowledges the financial support from the University of Minnesota through the 2015-16 Doctoral Dissertation Fellowship. The work of M. R. Jovanović was supported in part by the National Science Foundation under Award CMMI 1363266, the Air Force Office of Scientific Research under Award FA9550-16-1-0009, and the University of Minnesota Informatics Institute Transdisciplinary Faculty Fellowship.

J. Annoni and P. Seiler are with the Aerospace Engineering and Mechanics at the University of Minnesota, Minneapolis, MN 55455 USA (emails: anno0010@umn.edu, seiler@umn.edu).

M. R. Jovanović is with the Electrical and Computer Engineering at the University of Minnesota, Minneapolis, MN 55455 USA.

the linear channel flow problem described in Section III. The proposed approach will be compared to standard DMD in Section III-A. In addition, the impact of using sparsity-promoting DMD with exogenous inputs will be discussed. Section IV will end with some conclusions and future work.

II. Problem formulation

In this section, we describe a variant of dynamic mode decomposition that is applicable to systems with exogenous inputs. We obtain the optimal amplitudes of DMD modes as the solution of a least-squares problem and show how dominant modes can be identified. This requires the solution of a regularized least-squares problem, where a regularization term serves as a proxy for inducing sparsity. In contrast to standard sparsity-promoting DMD [24], it is necessary to induce block sparsity in the amplitudes that account both for the initial conditions and inputs.

A. Dynamic Mode Decomposition for Systems with Inputs

Consider a discrete-time nonlinear system

$$\psi_{t+1} = f(\psi_t, u_t)$$

where $\psi \in \mathbb{C}^n$ and $u \in \mathbb{C}^p$ are the state and input vectors, respectively. A collection of snapshots are obtained via simulations or experiments

$$\Psi_0 = \left[\begin{array}{cccc} \psi_0 & \psi_1 & \dots & \psi_{N-1} \end{array} \right] \in \mathbb{C}^{n\times(N-1)} \quad (1)$$

$$\Psi_1 = \left[\begin{array}{cccc} \psi_1 & \psi_2 & \dots & \psi_{N} \end{array} \right] \in \mathbb{C}^{n\times(N-1)} \quad (2)$$

$$U_0 = \left[\begin{array}{cccc} u_0 & u_1 & \dots & u_{N-1} \end{array} \right] \in \mathbb{C}^{p\times(N-1)} \quad (3)$$

where N is the number of snapshots. Our objective is to identify a linear dynamical system

$$\psi_{t+1} = A\psi_t + Bu_t \quad (4)$$

that optimally approximates available data.

The state matrices (A, B) have the dimensions compatible to those of (ψ, u). These matrices can be obtained to optimally approximate the snapshot data. However, this is intractable for large systems. For example, spatially-discretized models resulting from the Navier-Stokes equations can have millions of states. It is thus common to project the state onto a low-dimensional subspace in order to make the least squares problem tractable.

Let $U \in \mathbb{C}^{n\times r}$, with $r < n$, have columns that form an orthonormal basis for a projection subspace. A sub-optimal, but useful, choice for the projection subspace is given by the POD modes of the matrix Ψ_0. Specifically, the POD modes focus on capturing the most amount of energy in the data. The POD modes can be obtained using the singular value decomposition of $\Psi_0 = U\Sigma V^*$. The POD modes are contained in the columns of U and the relative energy of each mode is captured by the singular values (i.e., the matrix Σ). The state of the linear system can be approximated on a subspace defined by the first r POD modes of Ψ_0.

The reduced-order model is expressed in terms of the projected state, $\eta_t := U^*\psi_t \in \mathbb{C}^r$, and it is given by

$$\eta_{t+1} = (U^*AU)\eta_t + (U^*B)u_t := F\eta_t + Gu_t. \quad (5)$$

The matrices in the reduced-order representation have dimensions $F \in \mathbb{C}^{r\times r}$ and $G \in \mathbb{C}^{r\times p}$ and the matrices A and B in the original state-space model are determined by

$$\left[\begin{array}{cc} A & B \end{array} \right] \approx \left[\begin{array}{cc} UFU^* & UG \end{array} \right] = U \left[\begin{array}{cc} F & G \end{array} \right] \left[\begin{array}{cc} U^* & 0 \\ 0 & I_p \end{array} \right] \quad (6)$$

The optimal (reduced-order) state matrices on a subspace spanned by the columns of U are obtained as the solution to the least-squares problem

$$\underset{F,\,G}{\text{minimize}} \; \left\| \Psi_1 - U \left[\begin{array}{cc} F & G \end{array} \right] \left[\begin{array}{cc} U^* & 0 \\ 0 & I_p \end{array} \right] \left[\begin{array}{c} \Psi_0 \\ U_0 \end{array} \right] \right\|_F^2 \quad (7)$$

and they are determined by

$$\left[\begin{array}{cc} F_{\text{opt}} & G_{\text{opt}} \end{array} \right] = U_r^* \Psi_1 \left[\begin{array}{c} \Sigma_r V_r^* \\ U_0 \end{array} \right]^\dagger \quad (8)$$

where $\dagger$ denotes pseudo-inverse and U_r denotes the first r modes contained in U. We note that the dynamic matrix F_{opt} is, in general, different from the matrix F_{dmd} resulting from the standard DMD algorithm [15]. This method varies slightly from [25] in that the reduced-order state matrices are formed after projecting the data matrices onto a subspace spanned by the modes of Ψ_0. This is done to speed up the computation of the state matrices, F_{opt} and G_{opt}.

B. Optimal Amplitudes of DMD modes

The optimal amplitudes of the DMD modes resulting from the setup with external inputs are computed next. This results from the solution to the least-squares problem that is presented for standard DMD outlined in [24].

First, an eigenvalue decomposition of F can be used to construct modes at a specific temporal frequency

$$F = \underbrace{\left[\begin{array}{ccc} \xi_1 & \dots & \xi_r \end{array} \right]}_{Y} \underbrace{\left[\begin{array}{ccc} \mu_1 & & \\ & \ddots & \\ & & \mu_r \end{array} \right]}_{D_\mu} \underbrace{\left[\begin{array}{c} \zeta_1^* \\ \vdots \\ \zeta_r^* \end{array} \right]}_{Z^*} \quad (9)$$

where Y is a matrix that contains the left eigenvectors, Z is a matrix that contains the right eigenvectors, and D_μ contains the associated eigenvalues. The solution to the reduced-order system (5) is given by

$$\eta_t = F^t\eta_0 + \sum_{m=0}^{t-1} F^{t-m-1}Gu_m \quad (10)$$

$$= (YD_\mu^tZ^*)\eta_0 + \sum_{m=0}^{t-1}(YD_\mu^{t-m-1}Z^*)Gu_m \quad (11)$$

Equivalently, modal contribution of the initial condition and the input to the state η_t is captured by

$$\eta_t = \sum_{i=1}^{r} \xi_i\mu_i^t \underbrace{\zeta_i^*\eta_0}_{\alpha_i} + \sum_{m=0}^{t-1}\sum_{i=1}^{r} \xi_i\mu_i^{t-m-1} \underbrace{\zeta_i^*G}_{\beta_i^*} u_m \quad (12)$$

where α_i and β_i determine the contribution of the ith mode to the response.

The DMD modes can be expressed as $\phi_i := U_r \xi_i$ and the state of the full-order system can be approximated by

$$\psi_t \approx U_r \eta_t \tag{13}$$

Thus, the approximate solution to the full-order state can be written as

$$\begin{aligned}\psi_t &= U_r \left(\sum_{i=1}^{r} \xi_i \mu_i^t \alpha_i \right) + U_r \left(\sum_{m=0}^{t-1} \sum_{i=1}^{r} \xi_i \mu_i^{t-m-1} \beta_i^* u_m \right) \\ &= \sum_{i=1}^{r} \phi_i \mu_i^t \alpha_i + \sum_{m=0}^{t-1} \sum_{i=1}^{r} \phi_i \mu_i^{t-m-1} \beta_i^* u_m\end{aligned}$$

By expressing the matrix of snapshots Ψ_0 as

$$\Psi_0 = \Phi \sum_{i=1}^{r} \underbrace{\begin{bmatrix} \mu_i^t & \sum_{m=0}^{t-1} \mu_i^{t-m-1} u_m^* \end{bmatrix}}_{q_i^*(t)} \underbrace{\begin{bmatrix} \alpha_i \\ \beta_i \end{bmatrix}}_{x_i} \tag{14}$$

we clearly see that spectral coefficients α_i and β_i capture contribution of individual DMD modes. Note that columns of the matrix Φ are determined by the DMD modes ϕ_i. Equivalently, in the vector form we have

$$\underbrace{\begin{bmatrix} \psi_0 \\ \psi_1 \\ \vdots \\ \psi_{N-1} \end{bmatrix}}_{\tilde{\Psi}} = \begin{bmatrix} U_r \left(\sum_{i=1}^{r} \xi_i q_i^*(0) x_i \right) \\ U_r \left(\sum_{i=1}^{r} \xi_i q_i^*(1) x_i \right) \\ \vdots \\ U_r \left(\sum_{i=1}^{r} \xi_i q_i^*(N-1) x_i \right) \end{bmatrix} \tag{15}$$

or

$$\tilde{\Psi} \;=\; \mathrm{diag}(U_r)\, Q\, x$$

where $\mathrm{diag}(U_r)$ is a block-diagonal matrix containing the matrix U_r on the main diagonal and

$$Q \;=\; \begin{bmatrix} \xi_1 q_1^*(0) & \xi_2 q_2^*(0) & \dots & \xi_r q_r^*(0) \\ \xi_1 q_1^*(1) & \xi_2 q_2^*(1) & \dots & \xi_r q_r(1) \\ \vdots & & \ddots & \vdots \\ \xi_1 q_1^*(N-1) & \xi_2 q_2^*(N-1) & \dots & \xi_r q_r^*(N-1) \end{bmatrix}$$

and

$$x \;=\; \begin{bmatrix} x_1 \\ x_2 \\ \vdots \\ x_r \end{bmatrix}.$$

The vector of amplitudes of the DMD modes, x, can be found as the solution to the least-squares problem

$$\underset{x}{\text{minimize}} \quad J(x) := \left\| \tilde{\Psi} - \mathrm{diag}(U_r) Q x \right\|_2^2 \tag{16}$$

and it is determined by

$$x_{\mathrm{dmd}} \;=\; (Q^* Q)^{-1} Q^* \mathrm{diag}(U_r^*) \tilde{\Psi}. \tag{17}$$

C. Sparsity-Promoting DMD for Systems with Inputs

We next address the challenge of identifying a subset of DMD modes that strikes an optimal balance between fidelity to available data and model complexity. In contrast to POD modes, DMD modes are not orthogonal, and there is no natural ordering. We identify dominant modes by solving the regularized least-squares problem where the regularization term is introduced as a proxy for inducing sparsity. Our approach represents an extension of the sparsity-promoting DMD algorithm [24] with a difference that it is desired to promote block sparsity instead of elementwise sparsity.

Let us consider the regularized optimization problem

$$\underset{x}{\text{minimize}} \quad J(x) + \gamma \sum_{i=1}^{r} \|x_i\|_2 \tag{18}$$

where the Euclidean norm of the DMD amplitudes $g(x) := \sum_i \|x_i\|_2$ is introduced to promote block sparsity. A similar approach is typically used in statistics literature to drive a set of variables (in our case, coefficients α_i and β_i) jointly to zero.

Once this optimization problem is solved, a sparsity structure is fixed based on the non-zero coefficients that determine the contribution of each DMD mode to a particular snapshot. Specifically, the "polished" amplitudes are found by solving a constrained quadratic program

$$\begin{aligned} \underset{x}{\text{minimize}} \quad & J(x) \\ \text{subject to} \quad & E^T x = 0 \end{aligned} \tag{19}$$

where E provides information about the sparsity structure of the coefficients contained in x.

D. Alternating Direction Method of Multipliers Algorithm

The algorithm used to solve (18) is based on Alternating Direction Method of Multipliers (ADMM) [27]. We begin by rewriting the smooth part of the objective function in optimization problem (18) as

$$J(x) \;=\; \quad x^* P x - \tilde{q}^* x - x^* \tilde{q} \tag{20}$$

where $P := Q^* Q$ and $\tilde{q} = Q^* \mathrm{diag}(U_r^*) \tilde{\Psi}$. This is a convex optimization problem that can be solved using standard algorithms (e.g., ADMM). To bring the problem into a form amenable to ADMM, we introduce an auxiliary optimization variable z,

$$\begin{aligned} \underset{x,z}{\text{minimize}} \quad & J(x) \;+\; \gamma\, g(z) \\ \text{subject to} \quad & x - z = 0 \end{aligned} \tag{21}$$

and define the augmented Lagrangian

$$\begin{aligned} \mathcal{L}_\rho(x, z, \rho) \;:=\; & J(x) + \gamma g(z) \\ & + \frac{1}{2} \left(\lambda^*(x - z) + (x - z)^* \lambda + \rho \|x - z\|_2^2 \right). \end{aligned} \tag{22}$$

Here, λ is a vector of Lagrange multipliers and ρ is a positive parameter. ADMM minimizes the augmented Lagrangian

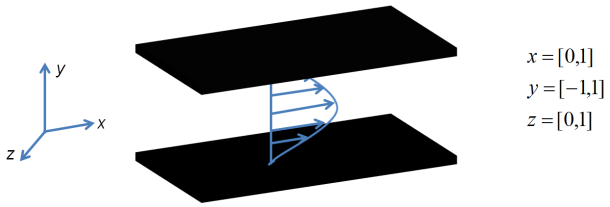

Fig. 1. Depiction of the channel flow problem.

separately with respect to x and z followed by a dual ascent update of the Lagrange multiplier λ,

$$\begin{aligned} x_{k+1} &= \underset{x}{\operatorname{argmin}}\ \mathcal{L}_\rho(x, z^k, \lambda^k) \\ z_{k+1} &= \underset{z}{\operatorname{argmin}}\ \mathcal{L}_\rho(x^{k+1}, z, \lambda^k) \\ \lambda^{k+1} &= \lambda^k + \rho\,(x^{k+1} - z^{k+1}). \end{aligned} \tag{23}$$

It can be shown that x and z can be explicitly updated

$$\begin{aligned} x^{k+1} &= (P + (1/\rho)I)^{-1}\left(\tilde{q} + \tfrac{\rho}{2}\left(z^k - \tfrac{1}{\rho}\lambda^k\right)\right) \\ z^{k+1} &= \begin{cases} \left(1 - \frac{a}{\|v^k\|_2}\right) v^k, & \|v^k\|_2 > a \\ 0, & \|v^k\|_2 < a. \end{cases} \end{aligned}$$

where $a = \gamma/\rho$ and $v^k = x^{k+1} + (1/\rho)\lambda^k$. These parameters provide thresholding for the ADMM algorithm.

III. Example: Linearized Channel Flow

We use the 3D incompressible linearized Navier-Stokes equations in a channel flow to illustrate our developments; see Fig. 1 for geometry. The application of the Fourier Transform in the streamwise (x) and the spanwise (z) directions along with the use of a pseudospectral method in the wall-normal direction yields the finite-dimensional state-space representation

$$\begin{aligned} \dot{\psi}(k_x, k_z, t) &= A(k_x, k_z)\psi(k_x, k_z, t) + \\ &\quad B(k_x, k_z)d(k_x, k_z, t) \end{aligned} \tag{24}$$

where ψ is the state and d is a spatially distributed and temporally varying body forcing. This system governs the dynamics of infinitesimal flow fluctuations around the parabolic velocity profile $U(y) = 1 - y^2$. In what follows, we fix the Reynolds number to $R = 2000$ and confine our attention to a pair of horizontal wavenumbers ($k_x = 1$, $k_z = 1$). In the wall-normal direction, we use 200 collocation points, resulting in 400 total states. This system is advanced in time and snapshots are recorded with $\Delta t = 1$. A random initial condition that satisfies proper boundary conditions in the wall-normal direction is used and all numerical computations are performed in MATLAB. For additional details about the linearized Navier-Stokes equations, we refer the reader to [28].

A. DMD vs. DMD with Exogenous Inputs

The reduced-order model of the channel flow problem was constructed using standard DMD and DMD with inputs (described in Section II-A) to demonstrate the benefit of adding an exogenous input to the system. For DMD with inputs, the system is excited for 100 seconds using a streamwise body forcing that enters as a temporal chirp excitation in the middle of the channel. This results in 100 snapshots that we use as a basis for system identification.

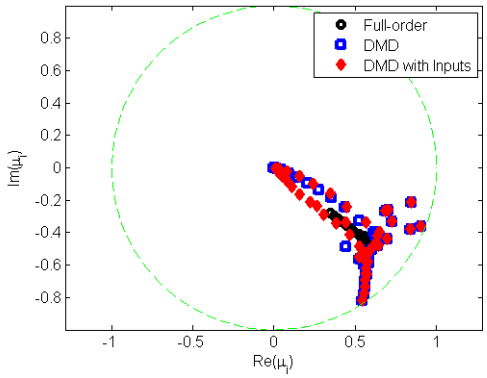

Fig. 2. Eigenvalues obtained with standard DMD and DMD with inputs.

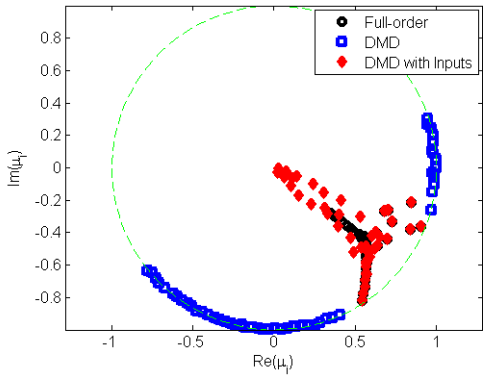

Fig. 3. Eigenvalues in the presence of noise with variance 10^{-5}.

Figure 2 shows the eigenvalues of the full-order A operator, the A operator identified by DMD, and the A operator identified by DMD with inputs. DMD with inputs can be used to identify the eigenvalues of the system in the same way as standard DMD. In addition, the input excitation provides additional energy to the system to aid in identifying the dynamics. In particular, DMD with inputs can handle small amounts of process noise. Process noise may have many interpretations. However, in this paper, process noise refers to the uncertainties and/or nonlinearities that are being neglected in the proposed dynamic equation. Figure 3 compares the eigenvalues resulting from standard DMD and DMD with inputs for the system subject to process noise with variance 10^{-5}. We see that DMD with inputs is significantly more robust than standard DMD. This is in concert with the results in system identification literature [8], where it has been shown that the choice of input plays an important role in the ability to characterize system's dynamics. Our ongoing efforts are direct towards establishing an analytical framework for our computational observations.

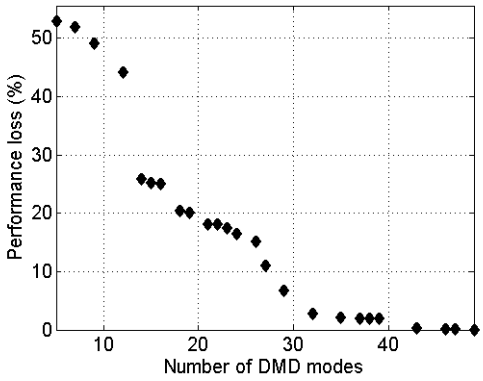

Fig. 4. Performance loss with respect to the number of DMD modes selected.

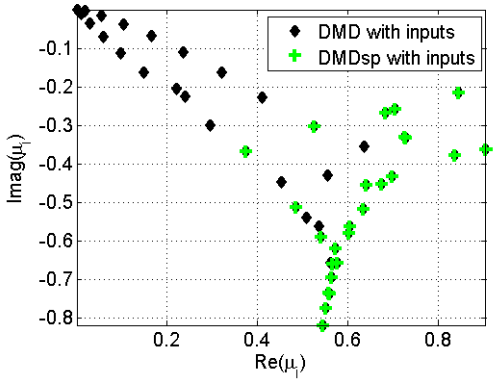

Fig. 5. Eigenvalues the are omitted when using the sparsity promoting approach. This is shown for $Nz = 31$.

B. Sparsity-Promoting DMD for Systems with Inputs

We next identify the dominant DMD modes using the sparsity-promoting DMD algorithm for systems with inputs. For this setup, the rank of the snapshots matrix, Ψ_0, is $r = 50$. The sparsity-promoting algorithm eliminates the DMD modes that have weak contribution to the available data.

Figure 4 shows the performance loss as the sparsity-promoting algorithm eliminates DMD modes. The performance loss is computed by:

$$PL(\%) := 100\sqrt{\frac{J(\alpha)}{J(0)}} \tag{25}$$

We see that there is minimal loss in performance using only 35 DMD modes ($< 1\%$). As the number of DMD modes get smaller the performance loss increases. For example, reducing the number of DMD modes to 25 introduces a 15% performance loss.

Figure 5 shows the eigenvalues that are preserved with 31 DMD modes. This number offers a performance loss of only 7%. The number of DMD modes retained is determined by the number of non-zero x_i vectors where each x_i vector contains the spectral coefficients associated with a particular mode. A vector, x_i is considered non-zero if at least one of its entries is non-zero. In other words, all of the elements of the vector x_i have to be zero for a DMD mode to be removed. These eigenvalues are associated with the DMD modes that can capture the essential dynamics of the system. It is an open challenge to identify the optimal form of the exogenous input in order to retain the most important DMD modes.

The tradeoff between model performance and the number of DMD modes kept can be analyzed by changing the regularization parameter γ. As γ increases, more emphasis is placed on sparsity rather than model performance. This is shown in Figs. 6 and 7. In particular, Fig. 6 demonstrates that as γ increases, the number of non-zero vectors x_i decreases. The number of non-zero vectors is associated with the number of DMD modes retained. As the number of DMD modes

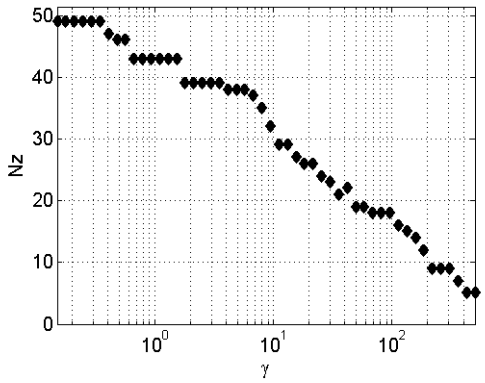

Fig. 6. Non-zero (Nz) x_i vectors as γ increases. The number of non-zero vectors correspond to the number of DMD modes retained.

decreases, it is expected that the performance of the reduced-order model also decreases. Fig. 7 shows the performance loss as γ increases. This indicates that increasing sparsity reduces quality of approximation of available snapshots.

IV. Concluding Remarks

The sparsity-promoting DMD technique has been extended to include exogenous inputs to the system. This approach was demonstrated on a the linear channel flow example and was compared to the standard DMD approach. It can be seen that the addition of an external input can improve the performance of the reduced-order model. Introducing sparsity to the DMD algorithm with inputs can decrease the order of the reduced-order model with minimal loss in model performance. The addition of an exogenous input to the system may impact the selectrion of DMD modes. The optimal choice of input will be investigated in future work. In addition, future work will focus on applying this approach to larger fluid dynamics problems.

References

[1] K. E. Johnson and N. Thomas, "Wind farm control: addressing the aerodynamic interaction among wind turbines," in *American Control Conference (ACC)*, pp. 2104–2109, IEEE, 2009.

[2] M. Churchfield and S. Lee, "NWTC design codes-SOWFA," 2012.

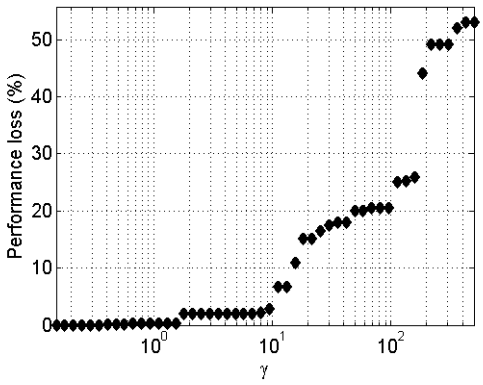

Fig. 7. Performance loss as γ increases.

[3] X. Yang, F. Sotiropoulos, R. Conzemius, J. Wachtler, and M. Strong, "Large-eddy simulation of turbulent flow past wind turbines/farms: the virtual wind simulator (VWiS)," *Wind Energy*, 2014.

[4] J. Beranek, L. Nicolai, M. Buonanno, E. Burnett, C. Atkinson, B. Holm-Hansen, and P. Flick, "Conceptual design of a multi-utility aeroelastic demonstrator," in *13th AIAA/ISSMO Multidisciplinary Analysis Optimization Conference*, pp. AIAA–2010–9350, 2010.

[5] R. Lind and M. Brenner, *Robust aeroservoelastic stability analysis*. Springer-Verlag, 1999.

[6] B. Danowsky, P. Thompson, C. Farhat, T. Lieu, C. Harris, and J. Lechniak, "Incorporation of feedback control into a high-fidelity aeroservoelastic fighter aircraft model," *Journal of Aircraft*, vol. 47, no. 4, pp. 1274–1282, 2010.

[7] K. Zhou, J. C. Doyle, and K. Glover, *Robust and optimal control*. Prentice hall New Jersey, 1996.

[8] M. Viberg, "Subspace-based methods for identification of linear time-invariant systems," *Automatica*, vol. 31, no. 12, pp. 1835–1851, 1995.

[9] G. Berkooz, P. Holmes, and J. Lumley, "The proper orthogonal decomposition in the analysis of turbulent flows," *Annual Review of Fluid Mechanics*, vol. 25, pp. 539–575, 1993.

[10] P. Holmes, J. Lumley, and G. Berkooz, *Turbulence, Coherent Structures, Dynamical Systems and Symmetry*. Cambridge University Press, 1988.

[11] M. Loéve, *Probability Theory*. Van Nostrand, 1955.

[12] C. Rowley, "Model reduction for fluids using balanced proper orthogonal decomposition," *International Journal of Bifurcation and Chaos*, vol. 15, no. 03, pp. 997–1013, 2005.

[13] K. Willcox and J. Peraire, "Balanced model reduction via the proper orthogonal decomposition," *AIAA journal*, vol. 40, no. 11, pp. 2323–2330, 2002.

[14] R. J. Adrian and J. Westerweel, *Particle image velocimetry*. No. 30, Cambridge University Press, 2011.

[15] P. Schmid, "Dynamic mode decomposition of numerical and experimental data," *Journal of Fluid Mechanics*, vol. 656, pp. 5–28, 2010.

[16] P. Schmid, L. Li, M. Juniper, and O. Pust, "Applications of the dynamic mode decomposition," *Theoretical and Computational Fluid Dynamics*, vol. 25, pp. 249–259, 2010.

[17] J. Tu, C. Rowley, D. Luchtenburg, S. Brunton, and J. Kutz, "On dynamic mode decomposition: Theory and applications," *submitted to the Journal of Computational Dynamics*, 2013.

[18] M. Budisic, R. M. Mohr, and I. Mezic, "Applied Koopmanism," *arXiv:1206.3164*, 2012.

[19] I. Mezic, "Analysis of fluid flows via spectral properties of the Koopman operator," *Annual Review of Fluid Mechanics*, vol. 45, pp. 357–378, 2013.

[20] C. W. Rowley, I. Mezić, S. Bagheri, P. Schlatter, and D. S. Henningson, "Spectral analysis of nonlinear flows," *Journal of fluid mechanics*, vol. 641, pp. 115–127, 2009.

[21] M. S. Hemati, M. O. Williams, and C. W. Rowley, "Dynamic mode decomposition for large and streaming datasets," *Physics of Fluids (1994-present)*, vol. 26, no. 11, p. 111701, 2014.

[22] S. Dawson, M. S. Hemati, M. O. Williams, and C. W. Rowley, "Characterizing and correcting for the effect of sensor noise in the dynamic mode decomposition," *arXiv preprint arXiv:1507.02264*, 2015.

[23] G. Iungo, C. Santoni-Ortiz, M. Abkar, F. Porté-Agel, M. Rotea, and S. Leonardi, "Data-driven reduced order model for prediction of wind turbine wakes," in *Journal of Physics: Conference Series*, vol. 625, p. 012009, IOP Publishing, 2015.

[24] M. R. Jovanović, P. J. Schmid, and J. W. Nichols, "Sparsity-promoting dynamic mode decomposition," *Physics of Fluids (1994-present)*, vol. 26, no. 2, p. 024103, 2014.

[25] J. Proctor, S. Brunton, and J. Kutz, "Dynamic mode decomposition with control," *arXiv:1409.6358*, 2014.

[26] F. Lin, M. Fardad, and M. R. Jovanovic, "Design of optimal sparse feedback gains via the alternating direction method of multipliers," *Automatic Control, IEEE Transactions on*, vol. 58, no. 9, pp. 2426–2431, 2013.

[27] S. Boyd, N. Parikh, E. Chu, B. Peleato, and J. Eckstein, "Distributed optimization and statistical learning via the alternating direction method of multipliers," *Foundations and Trends® in Machine Learning*, vol. 3, no. 1, pp. 1–122, 2011.

[28] M. R. Jovanovic and B. Bamieh, "Componentwise energy amplification in channel flows," *Journal of Fluid Mechanics*, vol. 534, pp. 145–183, 2005.